Polymer Journal (2016) 48, 863–867

www.nature.com/pj

ORIGINAL ARTICLE

Local and global conformations of flower micelles and flower necklaces formed by an amphiphilic alternating copolymer in aqueous solution

Kai Uramoto[1], Rintaro Takahashi, Ken Terao and Takahiro Sato

We investigated the local and global conformations of flower micelles and flower necklaces formed by the amphiphilic alternating copolymer of sodium maleate and dodecyl vinyl ether, P(MAL/C12), in an aqueous solution using small-angle X-ray scattering (SAXS) and light scattering. SAXS profiles obtained for seven P(MAL/C12) samples with different degrees of polymerization N_{01} showed sharp minima characteristic to the hydrophobic core formed by dodecyl groups with a low electron density. Both the SAXS profile $I(k)$ and hydrodynamic radius R_H for P(MAL/C12) samples with $N_{01} < 300$ are consistently explained by the flower micelle model with minimum-sized loops, while $I(k)$ for micelles formed by P(MAL/C12) samples with $N_{01} > 300$ is explained in terms of the flower necklace model, of which hydrophobic core size determined from $I(k)$ was slightly larger than that from R_H. The size distribution of the hydrophobic core is narrower for the flower necklace than for the flower micelle.
Polymer Journal (2016) **48,** 863–867; doi:10.1038/pj.2016.49; published online 25 May 2016

INTRODUCTION

Strauss and Jackson[1] were among the first to report the formation of polymer micelles by an amphiphilic polyelectrolyte (also called *a polysoap*) in aqueous solutions. However, they did not discuss the detailed conformation of the polymer micelle formed by the polysoap. More than 40 years later, Borisov and Helperin[2–6] proposed theoretical models of flower micelles, flower necklaces and bouquets of polymer micelles formed by polysoaps in aqueous solutions. Their models, however, have not been critically compared with experimental results using polysoap solutions over a long period of time.

Only recently, Kawata *et al.*[7] proposed a flower micelle model with minimum-sized loops and favorably compared this model with experimental results of the hydrodynamic radius for amphiphilic random copolymers in aqueous solutions. Afterward, Tominaga *et al.*[8] demonstrated that the radial distribution functions of the main chain, the hydrophobic side chain and the ionic group in an amphiphilic random copolymer micelle, generated by molecular dynamics simulations, were explained by the same flower micelle model with minimum-sized loops. More recently, Ueda *et al.*[9] investigated the micellar structure of the amphiphilic alternating copolymer of sodium maleate and dodecyl vinyl ether (P(MAL/C12); see Scheme 1) in aqueous solutions using static and dynamic light scattering (DLS) as well as time-resolved fluorescence, and found that a transition occurred from flower micelle to flower necklace upon increasing the degree of polymerization of the copolymer. Furthermore, they verified the validity of the flower micelle model with minimum-sized loops and the flower necklace model comprising the flower micelles to explain the experimental results obtained for the copolymer.

In the present study, we carried out small-angle X-ray scattering (SAXS) measurements on aqueous polysoap solutions to investigate the more local micellar structures of flower micelles and flower necklaces, choosing the amphiphilic alternating copolymer P(MAL/C12) as the polysoap. The SAXS profiles obtained were compared with the same models used by Ueda *et al.* We used a 0.04 M aqueous borax solution as the solvent for the SAXS measurements, instead of the 0.05 M aqueous NaCl used in a previous study,[9] because the pH of the test copolymer solutions can be controlled more easily.

EXPERIMENTAL PROCEDURE

Copolymer samples and test solutions

The seven P(MAL/C12) samples listed in Table 1 were used for the measurements that follow. The samples were the same as those used in a previous study, with the exception of the 320 k and 430 k samples,[9] and the two highest molecular weight samples were obtained from fractions that remained from the previous study. As performed previously, weight average molecular weights $M_{1,w}$ of the two new samples were determined in methanol containing 0.1 M $LiClO_4$ by static light scattering. Though molecular weight dispersity indices were not determined for the new samples, their molecular weight distributions may be considerably narrow, because the samples used in the previous study, which were fractionated in a similar way, have dispersity indices less than 2.[9]

Test solutions for SAXS as well as light scattering measurements were prepared according to the previous procedure.[7,9,10] Briefly, each freeze-dried

Department of Macromolecular Science, Osaka University, Toyonaka, Japan
[1]Current address: Sanyo Chemical Industries, Ltd., 11-1 Ikkyo Nomoto-cho, Higashiyama-ku, Kyoto 605-0995, Japan.
Correspondence: Professor T Sato, Department of Macromolecular Science, Osaka University, 1-1 Machikaneyama-cho, Toyonaka, Osaka 560-0043, Japan.
E-mail: tsato@chem.sci.osaka-u.ac.jp
Received 30 December 2015; revised 19 February 2016; accepted 15 March 2016; published online 25 May 2016

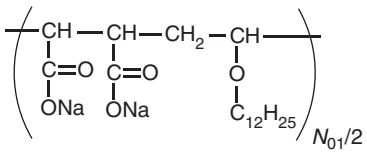

Scheme 1 Chemical structure of the alternating copolymer P(MAL/C12) used in this study.

Table 1 Molecular and micellar characteristics of P(MAL/C12) samples used in this study

Sample code	$M_{1,w}/10^4$[a]	$N_{01,w}$[b]	$M_w/10^4$[c]	$N_{0,w}$[d]	m_w[e]	A_2[f]	R_H (nm)[g]
14k	1.4[h]	76	6.10[i]	328	4.5	—	—
18k	1.8[h]	95	7.60	408	4.2	3.6	3.6
39k	3.9[h]	200	7.40	398	1.9	3.0	3.6
83k	8.3[h]	450	23.8	1280	2.9	0.39	6.5
300k	30[h]	1600	31.9	1720	1.1	0.76	7.8
320k	32	1700	34.8	1870	1.1	0.66	7.9
430k	43	2300	48.9	2630	1.1	2.0	9.7

[a]Weight average molecular weight of the samples in the Na salt form, in units of g mol^{-1}.
[b]Weight average degree of polymerization, calculated using the average monomer-unit molar mass $M_0 = 186$ g mol^{-1}.
[c]Weight average molar mass of the micelle in 0.04 M aqueous borax at 25 °C, in units of g mol^{-1}.
[d]Weight average number of monomer units per micelle.
[e]Weight average aggregation number of the micelle, calculated by $M_w/M_{1,w}$.
[f]Second virial coefficient of the micelle in 0.04 M aqueous borax at 25 °C, in units of 10^{-4} cm^3 mol g^{-2}.
[g]Hydrodynamic radius of the micelle in 0.04 M aqueous borax at 25 °C.
[h]Converted from $M_{1,w}$ of the acid form sample given in ref. 9.
[i]Assumed to be equal to M_w of the same sample in 0.05 M aqueous NaCl.[9]

copolymer sample was dissolved in pure water at room temperature, and heated at 90 °C for 30 min. The aqueous copolymer solution was then mixed with 0.08 M aqueous borax solution in a 1:1 volume ratio, and stirred overnight to afford the test solution with a borax molar concentration of 0.04 M and pH = 9.3, where the carboxylate groups of the copolymer were fully ionized.

Light scattering measurements

Static and dynamic light scattering measurements were also performed on 0.04 M aqueous borax solutions of P(MAL/C12) samples at 25 °C using an ALV/SLS/DLS-5000 light scattering instrument (ALV, Langen, Germany) with an Nd:YAG laser operating at 532 nm. The obtained data were analyzed by routine procedures.[9] The refractive index increment of P(MAL/C12) in 0.04 M aqueous borax was measured by a differential refractometer, and the result ($= 0.129$ cm^3 g^{-1}) was used to analyze the static light scattering data.

As in the previous study, some DLS data showed bimodal relaxations, which indicate that the solutions contained two scattering components with largely different sizes. In such cases, the scattering intensity of the major fast relaxation component in each solution was extracted from the total scattering intensity using the relaxation spectrum obtained by DLS and analyzed to determine the weight average molar mass M_w, the second virial coefficient A_2 and the hydrodynamic radius R_H of the major component, as performed in previous studies.[11,12] The results of M_w, A_2 and R_H for five P(MAL/C12) samples in 0.04 M aqueous borax are listed in Table 1. Because of the limited amount of sample, light scattering measurements were not made for the 14k sample; instead, the M_w of this sample in 0.04 M aqueous borax was assumed to be almost identical with that previously determined in 0.05 M NaCl. Weight average aggregation numbers m_w of the P(MAL/C12) micelles in 0.04M aqueous borax are also listed in Table 1.

SAXS measurements

SAXS measurements were carried out on the 0.04-M aqueous borax solutions of the P(MAL/C12) samples with copolymer mass concentrations of $c = 1.0 \times 10^{-3}$ g cm^{-3}, at the BL40B2 beamline of SPring-8 (Hyogo, Japan) and the BL-10C beamline of KEK-PF (Ibaraki, Japan). The wavelength, camera length and accumulation time at SPring-8 (KEK-PF) were chosen to be 0.10 nm (0.15 nm), 3170 mm (2040 mm) and 180 s (300 s), respectively. A capillary made of quartz containing a test solution or solvent was set in a heating block thermostated at 25 °C, and the intensity of the scattered X-ray was measured using an imaging plate detector, as a function of the magnitude k of the scattering vector. The excess scattering intensity $I(k)$ of each solution was calculated by subtracting the solvent intensity from that of the solution in the same capillary.

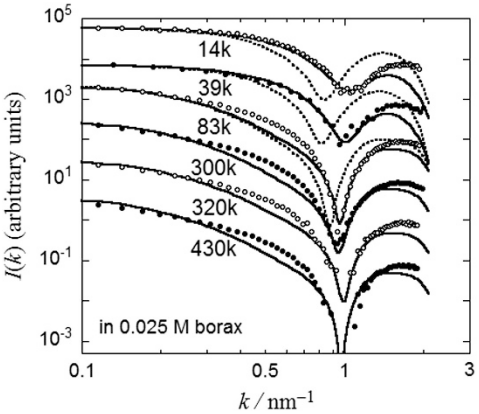

Figure 1 SAXS profiles for six P(MAL/C12) samples with different molecular weights in 0.04 M aqueous borax at 25 °C and pH = 9.3. The polymer mass concentration c was fixed to be 1.0×10^{-3} g cm^{-3}. Solid curves indicate fitting results calculated by the theory explained in the Discussion section. The data points and theoretical curves are shifted downward with increasing $M_{1,w}$.

RESULTS

Figure 1 shows the SAXS profiles of six P(MAL/C12) samples (listed in Table 1) in 0.04 M aqueous borax at 25 °C ($c = 1.0 \times 10^{-3}$ g cm^{-3}). All the profiles have a minimum and a maximum at ca. 1 nm^{-1} and 1.5 nm^{-1}, respectively. These SAXS profiles are characteristic of spherical micelles formed by low molar mass surfactants bearing a long alkyl group as the hydrophobe, for example, sodium dodecyl sulfate,[13] demonstrating the existence of a hydrophobic core with a low electron density, formed by the dodecyl groups in the micelle. It is noted that the minimum is sharper for P(MAL/C12) with $N_{01,w} > 300$, and the slope of the curve at the low k region increases with increasing $N_{01,w}$ at $N_{01,w} > 300$, indicating that P(MAL/C12) samples of higher $N_{01,w}$ form larger micelles.

The hydrodynamic radii R_H of P(MAL/C12) micelles obtained in 0.04 M aqueous borax (pH = 9.3; unfilled circles) is double logarithmically plotted against $N_{0,w}$ ($= N_{01,w} m_w$; the weight average number of monomer units per micelle) in Figure 2. Remarkably, all the unfilled circles are located below the dotted line passing through the filled circles, which represent data for the alternating copolymer of MAL and ethyl vinyl ether sodium (C2), in 0.05 M aqueous NaCl,[9] indicating that the shrinkage of the P(MAL/C12) chains occurred due to hydrophobic interactions among dodecyl groups. While two unfilled circles at the lowest $N_{0,w}$ are close to the theoretical curve (the dot–dash curve) previously obtained for the flower micelle model with minimum-sized loops in 0.05 M aqueous NaCl (pH = 10)[9] in the low $N_{0,w}$ region, the remaining unfilled circles at higher $N_{0,w}$ fall along a line with a slope that is similar to, but shifted downward from, the theoretical curve (the dot–dash curve) previously obtained for flower necklaces formed in 0.05 M aqueous NaCl.[9] Therefore, we can say that the 18k and 39k samples form uni-core flower micelles and that the

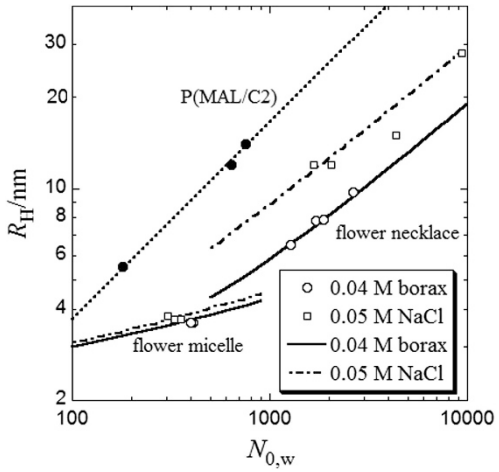

Figure 2 Double logarithmic plot of R_H against $N_{0,w}$ for P(MAL/C12) micelles in 0.04 M aqueous borax (unfilled circles), 0.05 M aqueous NaCl (squares) and for P(MAL/C2) in 0.05 M aqueous NaCl (filled circles) at 25 °C. The solid (dot–dash) curves indicate theoretical values calculated by the theory explained in the Discussion section for the flower micelle and flower necklace models in 0.04 M aqueous borax (0.05 M aqueous NaCl[9]).

83k, 300k, 320k and 430k samples form multi-core flower necklaces. Moreover, we conclude that the micellar structure of the flower necklace formed by higher molecular weight P(MAL/C12) may be sensitive to the solvent conditions.

As mentioned in our previous report,[9] there is an optimum number of monomer units to form the uni-core flower micelle, which is ca. 400 for the two lowest molecular weight samples in this study. If the degree of polymerization of the sample exceeds this optimum number, then two or more hydrophobic cores must be constructed. Thus, the uni-core to multi-core micelle transition takes place at this critical degree of polymerization.

DISCUSSION

Flower micelle and flower necklace models

Ueda *et al.*[9] previously proposed the uni-core flower micelle and multi-core flower necklace models with minimum-sized loops, as illustrated in Figure 3. The former is assumed to comprise n_{loop} minimum-sized loops with a contour length l_{loop} and a spherical hydrophobic core consisting of n_{C12} hydrophobes. The three parameters characterizing the flower micelle are related to each other by

$$n_{loop} = N_0 h / l_{loop}, n_{C12} = \lambda(n_{loop} + 1) \quad (1)$$

where N_0 is the number of monomer units of the flower micelle, h is the contour length per monomer unit (=0.25 nm for vinyl polymers) and λ is the number of hydrophobes included in the core at each root of the loop. It should be noted that n_{C12} is less than the total number of the dodecyl groups in the flower micelle. Using molecular dynamics simulations, Tominaga *et al.*[8] demonstrated that for an amphiphilic random copolymer the dodecyl groups attached to the loop chains existed outside the hydrophobic core.

Assuming that l_{loop} is determined by the main-chain stiffness, we calculate l_{loop} by

$$l_{loop} = 0.8 \times 2q \quad (2)$$

where q is the persistence length of the copolymer chain and 0.8 is the Kuhn segment number where the ring closure probability of the wormlike chain abruptly increases.[14] Furthermore, according to the wormlike chain statistics, the distance d_{loop} from the root to the top of the minimum loop is calculated by[14]

$$d_{loop} = 0.62q \quad (3)$$

On the other hand, the radius of the hydrophobic core R_{core} can be calculated by

$$\frac{4\pi}{3} {R_{core}}^3 = n_{C12} \upsilon_{C12} \quad (4)$$

where υ_{C12} is the volume of the hydrophobe (=0.35 nm^3 for the dodecyl group) and n_{C12} is calculated from N_0 using Equation (1). The radius R of the flower micelle can be calculated by

$$R = R_{core} + d_{loop} \quad (5)$$

The hydrodynamic radius R_H for the flower micelle is identified with R calculated by the above equation with $N_0 = N_{0,w}$ obtained experimentally.

The particle scattering function $P(k)$ of the uni-core flower micelle may be approximated to that of a concentric sphere where the inner and outer spheres correspond to the hydrophobic core and loop region, respectively. Thus, we can calculate $P(k)$ by[15]

$$P(k) = \left[\frac{\Delta\tilde{\rho}_c {R_{core}}^3 \Phi(kR_{core}) + R^3 \Phi(kR)}{\Delta\tilde{\rho}_c {R_{core}}^3 + R^3}\right]^2 \quad (6)$$

where the function $\Phi(y)$ and $\Delta\tilde{\rho}_c$ are defined by

$$\Phi(y) \equiv \frac{3(\sin y - y\cos y)}{y^3} \quad (7)$$

and

$$\Delta\tilde{\rho}_c \equiv \frac{\Delta\bar{\rho}_{core} - \Delta\bar{\rho}_{shell}}{\Delta\bar{\rho}_{shell}} \quad (8)$$

with the excess electron densities at the core region $\Delta\bar{\rho}_{core}$ and at the shell region $\Delta\bar{\rho}_{shell}$. R_{core} and R are calculated by Equations (4) and (5), respectively. We assume that dodecyl groups outside the hydrophobic core belong to the loop region.

Pedersen and Gerstenberg[16,17] formulated the particle scattering function for spherical micelles, where the coronal part is represented as an assembly of Gaussian chains, instead of as uniform electron density. Although this modification slightly affects the scattering function in the high k region,[15] we do not use this formulation because the loop chains of the flower micelle are not Gaussian.

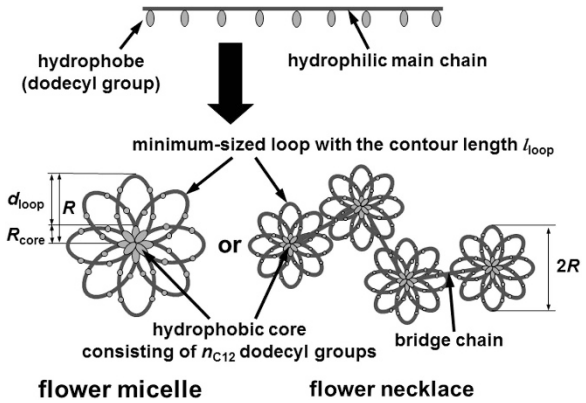

Figure 3 Schematic illustration of the flower micelle and flower necklace models used. The flower necklace can take bended conformations. A full color version of this figure is available at *Polymer Journal* online.

It is known that $P(k)$ has sharp minima and the sharpness strongly depends on the dispersity of the core radius, as observed from Equations (1) and (4). Assuming the dispersity of the core radius obeys the Gaussian distribution, we can calculate the average particle scattering function $P(k)$ by

$$P(k) = \frac{1}{\sqrt{\pi}} \int \left[\frac{\Delta\tilde{\rho}_c R'^3 \Phi(kR') + R^3 \Phi(kR)}{\Delta\tilde{\rho}_c R'^3 + R^3} \right]^2 \exp(-x^2)\,dx \tag{9}$$

where R' is defined by

$$R' \equiv \sqrt{2}\sigma x + R_{core} \tag{10}$$

with the mean value R_{core} and the variance σ^2 of the core radius. Furthermore, the scattering intensity $I(k)$ from the micellar solution with $c = 1.0 \times 10^{-3}$ g cm^{-3} may be affected by the inter-particle interference effect. This effect can be considered by

$$I(k) \propto \frac{N_0 P(k)}{1 + 2A_2 M_0 N_0 P(k) c} \tag{11}$$

using the second virial coefficient A_2 of the flower micelle;[18] M_0 is the molar mass of the monomer unit ($= 186$ g mol^{-1} for P(MAL/C12)).

The multi-core flower necklace may be viewed as a touched-beads wormlike chain consisting of n_c flower micelle units. Each flower micelle unit comprises N_u monomer units and possesses the radius R, given by Equation (5) along with Equations (1)–(4); in Equation (1), N_0 is replaced by N_u. The chain stiffness and excluded volume effect of the touched-beads wormlike chain are characterized in terms of the persistence length q_n and the excluded volume strength B_n, respectively. Yamakawa *et al.*[19] calculated the hydrodynamic radius R_H of the touched-beads wormlike chain as a function of n_c, R, q_n and B_n.[9] It is noted that the contour length of the touched-beads wormlike chain is given by $2Rn_c$.

The scattering function $P(k)$ of the flower necklace may be calculated by

$$P(k) \equiv P_u(k) P_{necklace}(k),$$
$$P_{necklace}(k) \equiv \frac{1}{{n_c}^2} \sum_{i=1}^{n_c} \sum_{j=1}^{n_c} \left\langle \frac{\sin(kr_{ij})}{kr_{ij}} \right\rangle \tag{12}$$

where $P_u(k)$ is the scattering function of the unit flower, r_{ij} is the center-to-center distance between beads (or unit flowers) i and j, and $\langle ... \rangle$ indicates the conformational average of the flower necklace. The scattering function $P_u(k)$ can be calculated by Equation (9), where N_0 in Equation (1) is replaced by N_u. The scattering function (or the structure factor) $P_{necklace}(k)$ for the discrete chain of n_c scattering centers, located on the wormlike chain contour has not been formulated thus far. Because the chain stiffness may not affect the local conformation or the scattering function in a high k region to an appreciable extent, we may approximate it to the scattering function for the random flight chain, where $\langle \sin(kr_{ij})/(kr_{ij}) \rangle = [\sin(2kR)/(2kR)]^{|j-i|}$.[20] The final expression of $P_{necklace}(k)$ can be written as

$$P_{necklace}(k) = \frac{n_c - 2x - n_c x^2 + 2x^{n_c+1}}{[n_c(1-x)]^2}, x \equiv \frac{\sin(2kR)}{2kR} \tag{13}$$

We also neglect the effect of the intra-chain excluded volume on $P_{necklace}(k)$, which is less important in the scattering function in a high k region. The scattering intensity $I(k)$ is calculated by Equations (11)–(13).

Comparison with experimental results

In Figure 2, the solid curves indicate the fitting results for R_H of P(MAL/C12) in 0.04 M aqueous borax (unfilled circles). The following paramers were chosen for both the flower micelle and the flower necklace: $q = 3$ nm and $\lambda = 3.5$; $N_u = 250$, $q_n = 7.1$ nm and $B_n = 4$ nm were used for the flower necklace model. The diameter $2R$ of the flower micelle unit within the flower necklace, calculated by Equation (5), is 6.9 nm. The value of q chosen was close to that of vinyl polyelectrolytes, including the electrostatic stiffness.[9] Data points at $N_{0,w} < 500$ (18k and 39k samples) and those at $N_{0,w} > 1000$ (for the 83k, 300k, 320k and 430k samples) are fitted to the theoretical curves for the flower micelle and flower necklace, respectively. The number of monomer units N_u ($= 250$) comprising the unit flower micelle is slightly smaller than that ($N_{0,w} \sim 400$; cf. Table 1) comprising the flower micelles of the 18k and 39k samples.

Data points for R_H of P(MAL/C12) in 0.05 M aqueous NaCl (unfilled squares) obtained in the previous study are fitted to the dot–dash curves drawn with $q = 3$ nm and $\lambda = 4.5$ for both the flower micelle and the flower necklace, and $N_u = 82$, $q_n = 5.9$ nm and $B_n = 2$ nm for the flower necklace model.[9] The difference between the solid and dot–dash curves for the flower necklace is mainly due to the values of N_u, but we have not yet specified the factor which determines N_u. We can only say that the factor may be related to solvent conditions, for example, the type of added salt in the aqueous solution.

The SAXS profiles shown in Figure 1 were also fitted by the above theory (Equations (6)–(13)) for the flower micelle (for the 14k and 39k samples) and the flower necklace (for the remaining samples) with $q = 3$ nm, $\lambda = 3.5$ and experimental A_2 listed in Table 1. The excess electron densities $\Delta\bar{\rho}_i$ in the core and shell regions are calculated by

$$\frac{\Delta\bar{\rho}_i}{N_A} = \left\{ \frac{n_{e,i}}{M_i} - \frac{\bar{v}_i}{v_{solv}} \left[\frac{n_{e,H_2O}}{M_{H_2O}} (1 - w_{borax}) + \frac{n_{e,borax}}{M_{borax}} w_{borax} \right] \right\} c_i, (i = \text{core and shell}) \tag{14}$$

where N_A is the Avogadro constant, n_e, M and $\bar{v}$ are the number of electrons, the molar mass and partial specific volume, respectively, of the component indicated by the subscript, v_{solv} and w_{borax} are the specific volume of the solvent and the weight fraction of the aqueous borax, respectively and c_i is the mass concentration in the core and shell regions. The parameters of the dodecyl group and MAL/C12 repeating unit of P(MAL/C12) are chosen as $n_{e,i}$, M_i and v_i of the core and shell, respectively. As the hydrophobic core region does not contain the solvent, $c_{core} = 1/\bar{v}_{core}$, and c_{shell} may be calculated by $[(3M_0N_u/4\pi N_A) - (R_{core}{}^3/\bar{v}_{core})]/(R^3 - R_{core}{}^3)$.

When the same parameters as those for R_H are selected for q, λ and N_u (that is, 3 nm, 3.5 and 250, respectively), minimum positions of the theoretical SAXS profiles deviated slightly toward lower k from those of the experimental profiles (cf. dotted curves for the 14k, 39k and 83k samples in Figure 1). Best fits were obtained, when slightly smaller values were chosen for R_{core} (cf. the last column of Table 2), as shown by the solid curves in Figure 1. The value of σ in Equation (10) determines the sharpness of the scattering function minimum; and the values in the seventh column of Table 2 were selected as σ to obtain the solid curves. Disagreements between theory and experimental results at $k > 1.3$ nm^{-1} may be due mainly to the uniform electron density assumption in the loop region of the flower micelle (cf. Equation (6)), but the local structure (for example, the thickness) of the copolymer chain may also contribute to the scattering function in such a high k region. The solid curves for the flower necklaces slightly deviate from the experimental profiles in an intermediate k region ($0.3 < k$ (nm^{-1}) < 0.7), and the deviations may arise from the neglect of the stiffness of the necklace chain, as mentioned above (cf. Equation (13)).

Table 2 Values of parameters characterizing flower micelles and flower necklaces selected at fitting for the SAXS profiles for P(MAL/C12) samples in 0.04 M aqueous borax

									R_{core} (nm)	
Sample code	*Micelle type*	n_c	q *(nm)*	λ	$N_{u,w}$	σ	$\Delta\tilde{\rho}_c$	R *(nm)*	*From Equation (4)*	*From SAXS*
14k	Flower micelle	1	3	3.5	330	0.39	-3.4_5	3.61	1.75	1.10
18k		1	3	3.5	410	—	—	3.74	1.87	—
39k		1	3	3.5	400	0.31	−3.2	3.72	1.86	1.30
83k	Flower necklace	5	3	3.5	250	0.06	-4.0_5	3.47	1.61	1.46
300k		7	3	3.5	250	0.08	-4.0_5	3.47	1.61	1.48
320k		7	3	3.5	250	0.07	-4.0_5	3.47	1.61	1.40
430k		11	3	3.5	250	0.04	-4.0_5	3.47	1.61	1.45

Abbreviation: SAXS, small-angle X-ray scattering.

The core size dispersity σ is much narrower for the flower necklace than that for the flower micelle. The hydrophobic core of the (unit) flower micelle should have an optimum aggregation number n_{C12} of dodecyl groups. While the uni-core flower micelle adjusts n_{C12} only by the polymer aggregation number m_w, the multi-core flower necklace can adjust this number by changing both m_w and the number of cores n_c. Thus, the flower micelle unit in the flower necklace may be able to approach the optimum n_{C12} more easily, which may be the reason for the sharper minimum of $I(k)$ of the flower necklace.

As demonstrated previously by the molecular dynamics simulation for the flower micelle formed by an amphiphilic random copolymer,[8] the radial distribution function of the dodecyl group $\rho_{C12}(r)$ is a gradually decreasing function of the radial distance (cf. Figure 4 of Ref. 8), and there exists a domain where the dodecyl groups intermingle with the copolymer main chain. As mentioned above, the size distribution of the hydrophobic core is broader for the flower micelle than that for the flower necklace, indicating that $\rho_{C12}(r)$ for the unit flower of the flower necklace may be a more sharply changing function and that the flower micelle model characterized by Equations (1)–(5) (where N_0 is replaced by N_u) is more suitable for the unit flower of the flower necklace. As the result, the R_{core} value calculated by Equation (4) is closer to that determined by the SAXS fitting (see Table 2).

CONCLUSION

We have investigated the local and global conformations of micelles formed by an amphiphilic alternating copolymer P(MAL/C12) in an aqueous solution using SAXS and light scattering. Both local and global conformations for micelles of P(MAL/C12) with $N_{01,w}$ (the weight average degree of polymerization) <300 and $N_{01,w}$ >300 have been explained consistently by the flower micelle and flower necklace models with minimum-sized loops, respectively, as previously proposed.[9] The characteristic minimum of the SAXS profile arising from the hydrophobic core of dodecyl groups indicates that the size and size distribution of the hydrophobic core are larger and narrower, respectively, for the flower necklace than for the flower micelle. These differences in the local hydrophobic core structure between the flower micelle and flower necklace are not reflected on the more global hydrodynamic radius.

CONFLICT OF INTEREST

The authors declare no conflict of interest.

ACKNOWLEDGEMENTS

This work was supported by JSPS KAKENHI Grant Number 23350055. We are grateful to Dr Yo Nakamura in Kyoto University, Dr Noboru Ohta in SPring-8 and Dr Nobutaka Shimizu in KEK for SAXS measurements. The synchrotron radiation experiments were performed at the BL40B2 in SPring-8 with the approval of the Japan Synchrotron Radiation Research Institute (JASRI) (Proposal #2012B1452, #2011A1049 and #2011A1925) and at the BL-10C in KEK-PF under the approval of the Photon Factory Program Advisory Committee (#2011G557).

1 Strauss, U. P. & Jackson, E. G. Polysoaps. I. Viscosity and solubilization studies on an n-dodecyl bromide addition compound of poly-2-vinylpyridine. *J. Polym. Sci* **6**, 649–659 (1951).
2 Borisov, O. V. & Halperin, A. Self-assembly of polysoaps. *Curr. Opin. Colloid Interface Sci.* **3**, 415–421 (1998).
3 Borisov, O. V. & Halperin, A. Polysoaps: extension and compression. *Macromolecules* **30**, 4432–4444 (1997).
4 Borisov, O. V. & Halperin, A. Micelles of polysoaps: the role of bridging interactions. *Macromolecules* **29**, 2612–2617 (1996).
5 Borisov, O. V. & Halperin, A. Micelles of polysoaps. *Langmuir* **11**, 2911–2919 (1995).
6 Halperin, A. in *Supramolecular Polymers* (ed. Ciferri A.) (Marcel Dekker, New York, Basel, 2000).
7 Kawata, T., Hashidzume, A. & Sato, T. Micellar structure of amphiphilic statistical copolymers bearing dodecyl hydrophobes in aqueous media. *Macromolecules* **40**, 1174–1180 (2007).
8 Tominaga, Y., Mizuse, M., Hashidzume, A., Morishima, Y. & Sato, T. Flower micelle of amphiphilic random copolymers in aqueous media. *J. Phys. Chem. B* **114**, 11403–11408 (2010).
9 Ueda, M., Hashidzume, A. & Sato, T. Unicore-multicore transition of the micelle formed by an amphiphilic alternating copolymer in aqueous media by changing molecular weight. *Macromolecules* **44**, 2970–2977 (2011).
10 Yamamoto, H., Hashidzume, A. & Morishima, Y. Micellization protocols for amphiphilic polyelectrolytes in water. How do polymers undergo intrapolymer associations? *Polym. J.* **32**, 745–752 (2000).
11 Hashidzume, A., Kawaguchi, A., Tagawa, A., Hyoda, K. & Sato, T. Synthesis and structural analysis of self-associating amphiphilic statistical copolymers in aqueous media. *Macromolecules* **39**, 1135–1143 (2006).
12 Kanao, M., Matsuda, Y. & Sato, T. Characterization of polymer solutions containing a small amount of aggregates by static and dynamic light scattering. *Macromolecules* **36**, 2093–2102 (2003).
13 Prévost, S., Wattebled, L., Laschewsky, A. & Gradzielski, M. Formation of monodisperse charged vesicles in mixtures of cationic gemini surfactants and anionic SDS. *Langmuir* **27**, 582–591 (2011).
14 Yamakawa, H. & Stockmayer, W. H. Statistical mechanics of wormlike chains. II. Excluded volume effects. *J. Chem. Phys.* **57**, 2843–2854 (1972).
15 Sanada, Y., Akiba, I., Hashida, S. & Sakurai, K. Composition dependence of the micellar architecture made from poly(ethylene glycol)-block-poly(partially benzyl-esterified aspartic acid). *J. Phys. Chem. B* **116**, 8241–8250 (2012).
16 Pedersen, J. S. & Gerstenberg, M. C. Scattering form factor of block copolymer micelles. *Macromolecules* **29**, 1363–1365 (1996).
17 Pedersen, J. S. Analysis of small-angle scattering data from colloids and polymer solutions: modeling and least-squares fitting. *Adv. Colloid Interf. Sci* **70**, 171–210 (1997).
18 Sato, T., Jinbo, Y. & Teramoto, A. Light scattering study of semiflexible polymer solutions. III. Multicomponent solutions. *Polym. J.* **31**, 285–292 (1999).
19 Yamakawa, H. *Helical wormlike chains in polymer solutions* (Springer-Verlag, Berlin, Heidelberg, 1997).
20 Kajiwara, K., Burchard, W. & Gordon, M. Angular distribution of Rayleigh scattering from randomly branched polycondensates. *Br. Polym. J.* **2**, 110–115 (1970).